Genetic approaches to the conservation of migratory bats: a case study of the eastern red bat (*Lasiurus borealis*)

Maarten Vonhof, Amy L. Russell

Documented fatalities of bats at wind turbines have raised serious concerns about the future impacts of increased wind power development on populations of migratory bat species. However, for most bat species we have no knowledge of the size of populations and their demographic trends, the degree of structuring into discrete subpopulations, and whether different subpopulations use spatially segregated migratory routes. Here, we utilize genetic data from eastern red bats (*Lasiurus borealis*), one of the species most highly affected by wind power development in North America, to (1) evaluate patterns of population structure across the landscape, (2) estimate effective population size (N_e), and (3) assess signals of growth or decline in population size. Using data on both nuclear and mitochondrial DNA variation, we demonstrate that this species forms a single, panmictic population across their range with no evidence for the historical use of divergent migratory pathways by any portion of the population. Further, using coalescent estimates we estimate that the effective size of this population is in the hundreds of thousands to millions of individuals. The high levels of gene flow and connectivity across the population of eastern red bats indicate that monitoring and management of eastern red bats must integrate information across the range of this species.

2   **Authors:**
3
4   Maarten J. Vonhof[1,2] and Amy L. Russell[3]
5
6   [1]Department of Biological Sciences, Western Michigan University, Kalamazoo, MI, USA
7
8   [2]Environmental and Sustainability Studies Program, Western Michigan University, Kalamazoo, MI,
9   USA
10
11 [3]Department of Biology, Grand Valley State University, Allendale, MI, USA
12
13
14 **Corresponding author:**
15 Maarten Vonhof
16 Dept. of Biological Sciences
17 Western Michigan University
18 1903 W. Michigan Avenue
19 Kalamazoo, MI 49008
20 Email: maarten.vonhof@wmich.edu
21 Tel: 269-387-5626
22 Fax: 269-387-5609

INTRODUCTION

As concerns about anthropogenic climate change and the long-term environmental impacts of burning

of fossil fuels on biological and human systems have heightened, there is increasing motivation to

develop alternative sources of energy that will reduce the production of greenhouse gasses. Wind

power has become an increasingly important sector of the energy industry and is one of the fastest

growing sources of renewable energy (Kaldellis & Zafirakis, 2011; Leung & Yang, 2012). Despite the

many positive aspects of wind power development, there have been environmental costs associated

with turbine installation and operation (Morrison & Sinclair, 2004; Abbasi et al., 2014). Fatalities of

bats at wind power installations have emerged as a major environmental impact of wind power

development, with large mortality events being reported at a number of wind energy facilities in the

United States and abroad (Erickson et al., 2001; Erickson, Johnson & Young, 2005; Kunz et al., 2007;

Arnett et al., 2008). The bat species most affected by wind power in North America are migratory, tree-

roosting species such as hoary bats (*Lasiurus cinereus*), eastern red bats (*Lasiurus borealis*), and silver-

haired bats (*Lasionycteris noctivagans*), which together constitute almost three-quarters of the bat

carcasses found at wind turbines (Arnett et al., 2008). Although mortalities may occur throughout April

to November, most bat fatalities in North America have been reported in late summer and early autumn

(reviewed by Kunz et al., 2007; Arnett et al., 2008) and appear to be concentrated during fall migration

of the affected species (Cryan, 2003).

The observed high levels of mortality for these species at wind power installations raise

concerns about the long-term impacts of this technology on bat populations, yet we lack the necessary

information to place this mortality in context with respect to baseline population estimates and

demographic trends of the affected species. For most bat species we have no knowledge of the size of

populations and their demographic trends, the degree of structuring into discrete subpopulations, and

whether different subpopulations use spatially segregated migratory routes. While estimates of local

48   population sizes within particular roosts may be feasible using traditional capture-mark-recapture

49   (CMR) methodology or survey techniques, no reliable range-wide population estimates exist for any

50   bat species (O'Shea & Bogan, 2003; Kunz et al., 2009). Traditional demographic approaches have

51   limitations when applied to bats, as they are nocturnal, exhibit cryptic behavior, and are difficult to

52   follow over time during extensive seasonal movements between summer breeding areas and

53   overwintering sites (Cryan, 2003; Rivers, Butlin & Altringham, 2006). The tree-roosting migratory bat

54   species that are killed in high numbers at wind turbines are especially inaccessible for traditional CMR

55   studies, given their solitary nature and restriction to forested habitats (Kunz, 1982; Shump & Shump,

56   1982a,b). Large-scale banding studies typically experience extremely low recapture rates (e.g., Glass,

57   1982; reviewed in O'Shea & Bogan, 2003), and there are serious data deficiencies with respect to sex-

58   and age-specific survival and reproductive rates that hamper our ability to widely apply demographic

59   models to bat populations. Given these difficulties, we require other approaches to estimating

60   population sizes and demographic trends within migratory bat populations affected by wind power

61   development.

62   Genetic approaches provide an alternative to traditional demographic methods of population

63   estimation, and allow us to estimate the degree of population structuring, demographic trends within

64   subpopulations, and effective population size (N_e) using data on allele frequencies or the base

65   composition of DNA sequences. Fewer individuals need to be sampled relative to CMR approaches,

66   and individuals need only be sampled a single time for many analyses. In addition, population

67   parameters can be estimated directly from the observed patterns of genetic variation, and age- or sex-

68   specific demographic information may not be required. Molecular markers can also be used to examine

69   levels of population differentiation within a species and to geographically delimit populations or

70   groups of populations based on the observed distribution of genetic variation (Freeland, Petersen &

71   Kirk, 2011). Importantly, such analyses can be used to define the relevant unit for population

72   monitoring, and highlight demographic connections among populations that may not be obvious from

73   behavioral data alone. As mating is likely to take place during migration in bats (Dodd & Adkins,

74   2007; Cryan, 2008; Cryan et al., 2012; Solick et al., 2012), gene flow should occur among populations

75   that interact during migration. Therefore it is likely that any genetically distinct populations, if they

76   exist, will be using different migratory pathways and may be subject to different mortality rates as

77   wind turbines are concentrated heterogeneously across the landscape. The analysis of genetic

78   population structure is therefore highly relevant to our understanding of bat – wind turbine interactions.

79   While it is not possible to directly estimate adult census population size (N_c) using molecular

80   data (although genetic markers can be used to identify individuals for traditional CMR analyses;

81   Luikart et al., 2010), it is possible to estimate effective population size (N_e). N_e is defined as the

82   number of individuals in an ideal Wright-Fisher population (a large, constant-sized, randomly-mating,

83   hermaphroditic population with discrete generations) that would lose genetic variation through genetic

84   drift at the same rate as the actual population (Crow & Denniston, 1988). It provides information on

85   how quickly genetic variation is being lost, or relatedness is increasing, in a population of interest, and

86   may be interpreted as an estimate of the number of individuals actually contributing genes to the next

87   generation. The estimation of N_e has seen wide application in studies of threatened or isolated

88   populations, as the magnitude of genetic drift, and hence loss of genetic variation, is inversely

89   proportional to N_e (Leberg, 2005; Wang, 2005; Luikart et al., 2010). Current estimates of N_e can be

90   used to assess the 'genetic health' of populations and their capability to respond to future

91   environmental change or anthropogenic changes via selection (Frankham, Ballou & Briscoe, 2002).

92   Estimation of N_e is also common in phylogeographic studies exploring past changes in population sizes

93   in relation to changing climatic conditions or vicariant events in the evolutionary history of species

94   (Avise, 2000; Russell et al., 2011), thus providing important insight into the demographic history of

95   populations and species.

96   Here, we utilize genetic data from eastern red bats (*Lasiurus borealis*), one of the species most

97   highly affected by wind power development in North America, to (1) evaluate patterns of population

98   structure and whether different subpopulations use spatially segregated migratory routes, (2) estimate

99   effective population size (N_e), and (3) assess signals of growth or decline in population size. This

100   species was chosen because it is one of the three bat species of greatest concern with regard to the

101   biodiversity impacts of wind energy, and has the highest fatality rate at a number of wind power

102   installations in the eastern United States (Arnett et al., 2008). Although estimates of census population

103   size would be preferable for understanding the size of bat populations and the potential impact of

104   fatalities at wind power installations, N_e estimates may provide us with valuable information on the

105   size of the evolutionarily relevant portion of the population (that portion contributing genes to the next

106   generation). Further, regular monitoring of N_e might serve as a proxy for tracking changes in

107   population size over time. Our study provides valuable data for understanding the population-level

108   impacts of mortalities due to wind power for this migratory bat species by assessing whether there are

109   discrete subpopulations that may represent independent management units and may undergo different

110   migratory behavior, whether populations from different regions may be connected demographically,

111   and the relative magnitude and historical population trends of the population or subpopulations we

112   identify.

113

114   **METHODS**

115   **Sampling**

116   Tissue samples from eastern red bats were collected by researchers capturing bats in the field or

117   collecting carcasses at wind power developments. We asked researchers across the range to collect

118   samples, but eastern red bats were not encountered in all areas due to regional differences in encounter

119   rates. Therefore, we have the largest sample sizes per site and the greatest number of samples from the

120   eastern portion of the species' range. All researchers were required to have appropriate state and

121   federal collecting permits. A small number of samples from Michigan were collected by one of the

122   authors (MJV) under permit from the state of Michigan (Michigan Department of Natural Resources

123   permit SC-1257) with appropriate Institutional Animal Care and Use Committee approval (Western

124   Michigan University protocol 05-03-01).

125   We compiled a collection of tissue samples from known sample sites collected in the summer

126   months (June to mid-August when bats are likely to be resident) primarily between 2000-2006, for the

127   purpose of assessing levels of genetic population structure and estimating N_e (Table 1, Table S1). We

128   received tissue samples for 1 – 39 bats from any given site. We had sufficient sample size ($N > 15$) for

129   each of 12 sites with which to carry out site-level population genetic analyses (Figure 1, Table 1).

130   Unlike colonial bats roosting in buildings or trees where bats can be captured in numbers from a single

131   point location during a single sampling session, tree-roosting bats such as eastern red bats are solitary.

132   Sampling these bats therefore must involve the capture of foraging individuals and may encompass

133   individuals from a wider area over a longer time scale. Therefore we define a 'site' as a collection of

134   capture localities within a set of nearby counties within a single state or province. For six of our sites,

135   bats were captured either within a single county or at a single capture location (AR, GA, MO, ON, TX,

136   WV-Ma), while the other six sites consisted of individuals captured in several counties within a given

137   state (IL, MD, MI, NC, TN, WV-Pe; the site label for the latter site represents one of the two counties

138   included; Table S1). There were no consistent differences in diversity measures within sites or levels of

139   differentiation between sites associated with sites containing samples from a single versus multiple

140   counties (see Results).

141   **Laboratory Methods**

142   Analyses of population genetic structure were carried out by analyzing variation at microsatellite loci

143   and mtDNA sequences. N_e estimation was carried out using these same markers, as well as sequences

144   from a nuclear intron marker. All but one analysis (msvar; see below) used this primary set of marker

145   data.

146   DNA was extracted from samples using a DNEasy Tissue Extraction Kit (Qiagen). Sixteen

147   variable microsatellite loci were genotyped for all individuals used in site-level analyses ($N = 284$)

148   using primers developed specifically for eastern red bats (primers Lbo-B06, C07, D08, D200, D202,

149   D203, D204, D226, D240, D245, and D248; Eackles & King, pers. comm.), as well as primers

150   originally developed for other bat species (MS3E10 and MS1C01, Trujillo & Amelon, 2009; IBat-

151   Ca22 Oyler-McCance & Fike, 2011; Cora_F11_C04, Piaggio, Figueroa & Perkins, 2009; and

152   Coto_G12F_B11R, Piaggio et al., 2009). Loci were multiplexed whenever possible; all PCR reactions

153   combined varying amounts of each primer and 2 μL template DNA with an illustra PuReTaq ready-to-

154   go PCR bead (GE Health Care) to a total volume of 25 μL (Table S2). The basic cycling conditions

155   consisted of 1 min at 94 °C, three cycles of 30 sec at 94 °C, 20 sec at T_a (54 or 60 °C), and 5 sec at

156   72□°C, 33 cycles of 15 sec at 94□°C, 20 sec at T_a, and 10 sec at 72 °C, followed by a final extension

157   at 72 °C for 30 min. Some amplifications required additional cycles or the removal of the final

158   extension step (Table S2). Multiple PCR reactions were subsequently pooled for loading on an

159   ABI3130 Sequencer at the Vanderbilt University DNA Sequencing Facility for fragment analysis (see

160   Table S2 for information on multiplexes and loads used), and visualized and scored using GeneMarker

161   software (SoftGenetics).

162   A fragment of the hypervariable 2 portion of the mitochondrial DNA control region (hereafter

163   HV2) was sequenced from 218 individuals used in site-level analyses (because of financial constraints

164   not all individuals from each location and not all locations were sequenced; Table 1), as well as 77 bats

165   from 30 additional locations that were not included in site-level analyses, for a total of 295 individuals

166   sequenced. Amplification of HV2 was initially carried out using the reverse complement of primer F

167 from Wilkinson & Chapman (1991; RevF: 5'-CTA CCT CCG TGA AAC CAG CAA C-3') sitting in

168 the central conserved sequence block as the forward primer, and the primer sH651 located in the

169 tRNA$_{Pro}$ gene (Castella, Ruedi & Excoffier, 2001) as the reverse primer. However, these primers span a

170 region containing a large stretch of 6 bp repeats, resulting in a large amplicon of 1500-2000 bp. We

171 therefore designed a new reverse primer (LABO-HV2R2: 5'-TCC TGT WAC CAT TAA YTA ATA

172 TGT CCC-3') that amplified a 408 bp fragment excluding the repeats. Amplification was carried out

173 using the above reaction conditions and the cycling conditions in Castella, Ruedi & Excoffier (2001)

174 with a T$_a$ of 60 °C. PCR reactions were cleaned using ExoSAP-IT (PCR Product Pre-Sequencing Kit,

175 Affymetrix), and sent to the University of Arizona Genetics Core for bi-directional sequencing.

176 Sequences were edited using CodonCode Aligner software (CodonCode Corporation). All unique HV2

177 haplotypes are deposited in Genbank (accession numbers KR337091 - KR337257; Table S1).

178   We further sequenced a 612 bp fragment of the nuclear Chymase intron 4 (CHY) for a random

179 subset of 88 individuals. Based on our results indicating panmixia across the sampled range of eastern

180 red bats (see Results), a random sample of individuals should represent genetic variation found in the

181 wider population (Felsenstein, 2006). This reduced subsample was chosen because the methods used

182 for N_e estimation are computationally intensive, and analysis would not have been possible with a

183 larger sample of sequences. CHY was amplified through PCR using the primers Chy-F (5'-GTC CCA

184 CCT GGG AGA ATG TG-3') and Chy-R (5'-TGG GAG ATT CGG GTG AAG-3'; Venta et al.,

185 1996). The reaction conditions were identical to those for the microsatellite loci, except that the

186 reaction used just 1 μL of template. The temperature profile included an initial extended denaturation

187 of 95 °C for 5 minutes, followed by 40 cycles of 95 °C for 1 minute, 52 °C for 1 minute and 72 °C for

188 1.5 minutes, with a final extension step at 72 °C for 4 minutes. The PCR reaction was cleaned using a

189 PCR purification kit (Qiagen) and sent to the University of Arizona Genetics Core for bi-directional

190 sequencing using the Chy-F and Chy-R primers. These diplotypes were edited and heterozygous sites

191 called using Sequencher v.4.8 (GeneCodes).

192 Some individuals ($N = 36$) found to contain two or more heterozygous sites were cloned using

193 the TOPO TA cloning kit (Life Technologies) following manufacturer's instructions. Six to eight

194 colonies were picked for each cloned individual. The picked colonies were each suspended in 10 μL

195 dH$_2$O and heated to 95°C for 10 minutes to lyse the cells. The cell lysate was then used directly as

196 template DNA for colony screening through PCR. The PCR reaction combined 10 ng of each primer

197 and 10 μL cell lysate with an illustra PuReTaq ready-to-go PCR bead (GE Health Care) to a total

198 volume of 25 μL. The temperature profile followed that described above for the initial cloned PCR.

199 PCR reactions yielding amplicons of the expected size (~650 bp) were cleaned using ExoSAP-IT

200 (Affymetrix) following the manufacturer's instructions. Cleaned PCR amplicons were then sent to the

201 University of Arizona Genetics Core for bi-directional sequencing using the Chy-F and Chy-R primers.

202 Based on these experimentally-resolved haplotypes, another 44 individuals with ambiguous diplotypes

203 were computationally phased using Phase v.2.1.1 (Stephens, Smith & Donnelly, 2001; Stephens &

204 Donnelly, 2003) with a confidence threshold of 0.95. All unique CHY haplotypes are deposited in

205 Genbank (accession numbers KR362302 - KR362477; Table S1).

206 **Analysis of Genetic Structure**

207 For microsatellite genotypes, deviations from Hardy-Weinberg equilibrium (HWE) at each locus were

208 estimated using GENODIVE (Meirmans, 2012), and loci were confirmed to be in linkage equilibrium

209 using FSTAT v.2.9.3 (Goudet, 1995). Null allele frequencies for each locus were estimated in

210 CERVUS v.3.1 (Kalinowski, Taper & Marshall, 2007). To test for differences among sites in levels of

211 genetic diversity, several indices of nuclear genetic diversity were estimated, including number of

212 alleles per locus, allelic richness, and the inbreeding coefficient (F_{IS}) using FSTAT, private allelic

213 richness using HP-RARE 1.0 (Kalinowski, 2005), and observed and expected heterozygosity using

214   GENODIVE. We then tested for differences among sites (or groups of sites) in allelic richness, and F_{IS}

215   in FSTAT, and expected heterozygosity in GENODIVE, using 10,000 permutations.

216   Different clustering algorithms can produce different solutions, and concordance among

217   multiple techniques is suggestive of the presence of a strong genetic signal (Guillot et al., 2009).

218   Therefore, we applied two different approaches to determine the most likely number of distinct genetic

219   clusters independent of original sampling locations. First, we utilized the model-based Bayesian

220   clustering approach in STRUCTURE v.2.3.3 software (Pritchard, Stephens & Donnelly, 2000; Falush,

221   Stephens & Pritchard, 2003) with population membership as a prior (Hubisz et al., 2009). To determine

222   the optimal number of clusters (K), we ran 10 runs per K, for $K = 1–10$, each with an MCMC search

223   consisting of an initial 100,000-step burn-in followed by 400,000 steps using the admixture model with

224   correlated allele frequencies. The most likely number of clusters was determined using the Evanno,

225   Regnaut & Goudet (2005) method implemented in the program STRUCTURE HARVESTER (Earl &

226   vonHoldt, 2012). The Evanno, Regnaut & Goudet (2005) method is not informative for the highest and

227   lowest K values; therefore, if the highest log likelihood value was observed for $K = 1$ or 10 across all

228   replicates, we accepted that as the best-supported value of K.

229   Second, we applied the repeated allocation approach of Duchesne & Turgeon (2009, 2012)

230   implemented in the software FLOCK. In this method, samples are initially randomly partitioned into K

231   clusters ($K \geq 2$), allele frequencies are estimated for each of the K clusters, and each genotype is then

232   reallocated to the cluster that maximizes the likelihood score. Repeated reallocation based on

233   likelihood scores (20 iterations per run) results in genetically homogeneous clusters within a run

234   (Duchesne & Turgeon, 2012). Fifty runs were carried out for each K, and at the end of each run the

235   software calculated the log likelihood difference (LLOD) score for each genotype (the difference

236   between the log likelihood of the most likely cluster for the genotype and that of its second most likely

237   cluster) and the mean LLOD over all genotypes. Strong consistency among runs (resulting in 'plateaus'

238   of identical mean LLOD scores) is used to indicate the most likely number of clusters (Duchesne &

239   Turgeon, 2012).

240   The level of genetic differentiation among pre-defined sites ($N = 12$; Table 1) based on

241   microsatellites was determined by calculating pairwise distance measures, including F_{ST} (Weir &

242   Cockerham, 1984) in ARLEQUIN v.3.11 (Excoffier, Laval & Schneider, 2005), and a measure

243   independent of the amount of within-site diversity (Jost's D; Jost, 2008) in GENODIVE. We tested for

244   significance of pairwise F_{ST} values between sites with 10,000 permutations, and performed an analysis

245   of molecular variance (AMOVA; Excoffier, Smouse & Quattro, 1992) to describe the relative amount

246   of genetic variation within and among sites in ARLEQUIN.

247   To describe overall levels of mtDNA diversity within sites, we calculated haplotype (h) and

248   nucleotide (π) diversities in DnaSP v.5.10.1 (Librado & Rozas, 2009). We calculated pairwise F_{ST}

249   values between sites and tested for significance with 10,000 permutations in ARLEQUIN to identify

250   pairs that were genetically distinct. As with microsatellite genotypes, we performed an AMOVA on

251   HV2 haplotype frequencies in ARLEQUIN.

252   **Estimation of N_e**

253   We used a number of approaches to estimate N_e for eastern red bats. Although we originally set out to

254   estimate the short-term variance effective population size (N_{eV}, Crandall, Posada & Vasco, 1999), it

255   quickly became apparent that N_e was very large (see Results). This constraint precluded the use of

256   single sample estimators based on linkage disequilibrium or summary statistics (Waples & Do, 2009;

257   Waples & Do, 2010; Tallmon, Luikart & Beaumont, 2004; Tallmon et al., 2008), which are only

258   effective for $N_e < 1,000$, or temporal methods (e.g., Jorde & Ryman, 1995), which are based on

259   changes in allele frequencies due to genetic drift between time points (as drift is negligible with large

260   N_e). Furthermore, the cohort-based demographic data required for the Jorde & Ryman (1995) method

261 were simply not available for any bat species.

262   Therefore, we focused on coalescent analyses, using three primary methods to estimate long-

263 term inbreeding effective population size (N_{eI}, Crandall, Posada & Vasco, 1999). These methods utilize

264 different types of data, and therefore provide complementary estimates based on differences in the

265 mutation rates of the markers used and differences in the underlying models assumed.

266 1. IMa2

267   We used the coalescent-based software IMa2 (release date 27 August 2012; Hey, 2010a, b) to

268 estimate the effective size of the panmictic eastern red bat population (see Results). The analysis

269 included the CHY and HV2 sequences and 16-locus microsatellite genotypes. One hundred

270 microsatellite genotypes (= 200 chromosomes) for each locus were subsampled at random out of the

271 full dataset in order to reduce the computational time of the analysis. The DNA sequence data (CHY

272 and HV2) were edited to conform to an infinite sites model of mutation; microsatellite data were

273 analyzed assuming a single-step model of mutation.

274   In the IMa2 analysis, we modified the underlying population model to consider only a single

275 population, with a uniform prior on the size of that population varying from $\theta = 0.05$ to 99.95. We ran

276 40 heated chains for an initial burn-in of ~3.6 million steps, followed by an MCMC search of ~10.2

277 million steps. Stationarity of the search chains was validated by monitoring ESS values.

278 2. Lamarc

279   We used the software package Lamarc v.2.1.8 (Kuhner, 2006) to estimate effective population

280 size and population growth rates independently for the nuclear CHY and the mitochondrial HV2

281 sequence data. We considered a model of a single panmictic population that undergoes population size

282 change (growth or decline) until it reaches the current population size. We implemented a Bayesian

283 analysis in Lamarc with priors on θ ranging from 10^{-5} to 50 and on the population size change

284 parameter (g) ranging from -500 to 2000. The data were analyzed in three independent runs, with each

285   run consisting of an MCMC search that was 20 million steps long and sampled every 200 steps. The

286   first 2 million steps were discarded as a burn-in. Each MCMC search was run as 3 heated chains, with

287   relative heating temperatures of 1, 1.5, and 3, and each search was replicated three times internally

288   within each of the independent runs. Posterior distributions for each independent run and for overall

289   results per locus were visualized using Tracer v.1.5. Results are reported as median point estimates

290   with 95% confidence intervals. All parameter estimates were well supported, with ESS values

291   exceeding 100 in all cases. N_e was calculated from the estimated coalescent-scaled parameter θ using

292   the equations: $\theta = N_e\mu$ for mitochondrial data and $\theta = 4N_e\mu$ for autosomal data, where N_e is the

293   effective size of the entire population. This software uses mutation rates in units of substitutions per

294   site per generation; based on the relative mutation rates estimated for the same data in the IMa2

295   analysis, we used a mutation rate of 4.29×10^{-8} per site per generation for the HV2 dataset and $7.76 \times$

296   10^{-9} per site per generation for the CHY dataset.

297   3. msvar

298   The third approach we used was the coalescent-based software msvar v.1.3 (Beaumont, 1999),

299   which estimates effective population size and demographic trends from microsatellite genotype data.

300   This analysis considers a model in which a single ancestral population of size N_A experiences

301   exponential population size change beginning at time t until the population reaches the current size N_1.

302   Unlike IMa2 and Lamarc, which calculate only long-term average N_e, msvar separately calculates

303   current and ancestral N_e. Therefore, rather than use the microsatellite genotypes included in all other

304   site-level analyses (which spanned a multi-year period), we generated microsatellite genotypes

305   following the methods outline above for two specific years for which we had sufficiently large sample

306   size (2002: $N = 353$ and 2010: $N = 226$). These datasets were analyzed separately to determine whether

307   mortality over that time interval had a measurable effect on estimates of N_e. Samples of genotypes for

308   2002 and 2010 were each comprised of a mixture of individuals of known summer origin, as well as

309   bats of unknown origin killed at wind power developments during fall migration.

310   To make the msvar analysis computationally feasible, we randomly subsampled 100 diploid

311   individuals from each time point (2002 and 2010). Subsampling was performed twice, producing

312   subsamples A and B for each time point, to ensure that no bias was introduced through subsampling.

313   Each analyzed dataset thus included 100 sixteen-locus genotypes (= 200 chromosomes) from a single

314   year (2002 or 2010).

315   The msvar analysis requires the specification of hyperpriors for each of the four parameters, N_1,

316   N_A, t, and the mutation rate μ. These hyperpriors describe distributions from which the locus-specific

317   initial parameter values are drawn, and are given here as [$\log_{10}(N_1)$, $\log_{10}(N_A)$, $\log_{10}(\mu)$, $\log_{10}(t)$]. The

318   parameter means were assumed to be normally distributed with means (7, 7, -3.5, 4.3) and standard

319   deviations (3.5, 4, 0.5, 2). We chose these values for (1) N_1 based on estimates of N_e for eastern red

320   bats from our own Lamarc analyses with a relatively large standard deviation to reflect our own

321   uncertainty regarding this parameter, (2) N_A based on a null hypothesis of no change in population size

322   with a larger standard deviation to accommodate increased uncertainty in historical parameters, (3) μ

323   based on Storz & Beaumont's (2002) msvar analysis of microsatellite variation in *Cynopterus* fruit

324   bats, and (4) t based on a hypothesis of population size change associated with the Last Glacial

325   Maximum with a relatively large standard deviation to reflect our own uncertainty regarding this

326   parameter. The parameter standard deviations were assumed to be normally distributed with means (0,

327   0, 0, 0) and standard deviations (0.5, 0.5, 2, 0.5). The means of the parameter standard deviations were

328   set to 0 to start the search algorithm with no inter-locus variation; the standard deviations of the

329   parameter standard deviations followed recommendations of Storz & Beaumont (2002). Each of the

330   four datasets (2 time points, with 2 subsamples each) were analyzed 2-3 times, with each run lasting

331   ~750 million to 2 billion steps and output logged every 100,000 steps. The initial 10% of the MCMC

332   chains from each run were excluded as a burn-in.

333

334   **RESULTS**

335   **Genetic Structure**

336   All microsatellite loci were unlinked and the majority of loci met HWE expectations in most

337   populations. MS3E10 was out of HWE in 2 of 12 sites (MO, ON), IBat Ca22 in 2 sites (GA, IL),

338   LboD202 in one site (AR), LboD204 in one site (WV-Pe), and LboD226 in 3 sites (GA, MI, WV-Ma).

339   Mean observed and expected heterozygosities within sites were high (0.82 and 0.88, respectively), as

340   was the mean number of alleles per locus (14.77) and allelic richness (12.92), although private allelic

341   richness was low (0.78; Table 1), and there were no significant differences among sites in allelic

342   richness, F_{IS}, or expected heterozygosity ($P > 0.05$ in all cases). Diversity statistics per locus are

343   presented in Table S3. Null allele frequencies per locus were generally low and < 0.1, except for locus

344   LboD226 with a frequency of 0.123 (Table S3). F_{ST} estimates with null alleles are unbiased in the

345   absence of population structure (Chapuis & Estoup, 2007), and removing loci that failed to meet HWE

346   in some sites from the analyses made no difference in our conclusions; therefore we present analyses

347   with all loci included.

348   AMOVA analysis of microsatellite genotypes indicated an almost complete lack of structure

349   ($F_{ST} = 0.0044$, $P < 0.001$), with pairwise F_{ST} and Jost's D values between populations consistently low

350   and non-significant (Table 2; F_{ST} range: -0.005 – 0.009; Jost's D range: -0.036 – 0.068). Log likelihood

351   values for $K = 1$ and $K = 2$ in the Bayesian clustering method (STRUCTURE) were nearly identical

352   (Table S4), and there was no basis upon which to conclude that the most likely number of clusters was

353   different from $K = 1$ given the low F_{ST} values among all sampled sites. Similarly, the repeated

354   reallocation clustering method (FLOCK) failed to reach a plateau for any $K > 1$, indicating $K = 1$ as the

355   most likely number of genetic clusters.

356   We observed 167 unique haplotypes representing 84 segregating sites among the 295

357   individuals sequenced at the mitochondrial HV2 locus. The number of haplotypes per site ranged from

358   13-23 (mean = 18.6), and haplotype diversity (h, mean = 0.986, range = 0.961 – 1) was high for all

359   sites (Table 1). However, nucleotide diversity (π, mean = 0.011, range = 0.009 – 0.016) was relatively

360   low for all sites (Table 1). AMOVA analysis indicated very low levels of mitochondrial differentiation

361   among sites (F_{ST} = 0.0113, $P < 0.05$; 1.13% of the variation is explained by differences among

362   sampling sites, and 98.87% of the variation occurs within sites). Accordingly, pairwise F_{ST} values

363   among sites were consistently low and ranged from -0.03 – 0.049 (Table 3), with only two significant

364   values (between the IL and MO and the IL and TX sites).

365   *N_e Estimation*

366   We used three coalescent methods to estimate N_e for eastern red bats: IMa2, Lamarc, and msvar. These

367   methods utilize different suites of data (microsatellites only for msvar, nuclear and mitochondrial

368   sequence data only for Lamarc, all three data types for IMa2), and therefore were expected to provide

369   complementary estimates based on differences in the mutation rates of the markers used and

370   differences in the underlying models assumed.

371   *IMa2*

372   This analysis converged on an unambiguous, unimodal posterior distribution for the single population

373   parameter θ (= $4N_e\mu$) for the panmictic eastern red bat population. The most probable value of θ was

374   estimated to be 37.95 (95% CI: 32.15 – 45.55). We used Pesole et al.'s (1999) estimate of mammalian

375   mitochondrial mutation rates (= 2.740×10^{-8} substitutions per site per year) to calculate locus-specific

376   mutation rates for our data. The geometric mean of these rates (= 8.03×10^{-6} substitutions per locus per

377   year = 1.61×10^{-5} substitutions per locus per generation; Table S5) was used to convert coalescent-

378   scaled estimates of θ into estimates of N_e. Our analysis thus supports an effective population size of

379   approximately 5.91×10^5 individuals (95% CI: $5.00 - 7.09 \times 10^5$; Figure 3).

380   *Lamarc*

381   We used coalescent-based analyses in Lamarc to provide estimates of θ and population growth

382   independently for the nuclear CHY and mitochondrial HV2 loci. Analyses of both markers provided

383   unambiguous, unimodal posterior probability distributions for both parameters. Utilizing the relative

384   mutation rates estimated from IMa2, estimates of N_e using HV2 across three runs in Lamarc were 5.18

385   $\times 10^5$ (95% CI: $4.25 - 7.22 \times 10^5$; Table 4). The estimate of N_e using CHY (males and females) was

386   significantly larger, with a mean of 1.52×10^6 (95% CI: $1.05 - 2.18 \times 10^6$; Table 4). There was a clear

387   signal of historical population growth recovered from both loci (Table 4); however, the time scale over

388   which this growth occurred is not estimated in the Lamarc model.

389   *msvar*

390   Although we found considerable variation from run to run, there were some clear patterns that emerged

391   from these analyses. Importantly, we found no consistent difference between parameter estimates from

392   the 2002 vs. 2010 time points (Figure 2; Figures S1-S2). We also found no consistent difference

393   between independent subsamples (A vs. B, each run 2-3 times) of the full dataset (runs A1-A3 vs. B1

394   and B3 for 2002; runs A1-A3 vs. B1-B3 for 2010). For the current effective population size N_1, we

395   recovered generally consistent estimates on the order of 10^4-10^5 (average $N_1 \approx 74,500$). Estimates of

396   ancestral effective population size N_A were less consistent among runs, but did result in estimates

397   ranging in the same order of magnitude as N_1 (average $N_A \approx 194,300$; Figure S1). These analyses

398   yielded differing signals of population growth vs. decline between runs (Table 5), although a majority

399   of runs (8 of 11) support a model of population decline rather than growth. The time of this population

400   size change (t) was also variable among runs, but generally was on the order of 10^3-10^4 years (average t

401 ≈ 21,600 years; Table 5, Figure S2). While the time of population size change is difficult to pinpoint

402 with great accuracy, these analyses clearly are not informative regarding very recent population size

403 change.

404

405 **DISCUSSION**

406 We observed extremely low levels of population structure and effective panmixia across the sampled

407 sites for eastern red bats using both nuclear and mitochondrial DNA markers. Furthermore, there is no

408 evidence for the historical use of different migratory pathways and no evidence for any barriers to gene

409 flow among any of the sampled localities. Few geographic barriers to the movement of vagile

410 organisms such as bats exist east of the Rocky Mountains, and therefore there are likely few

411 impediments to the movement of individuals across the landscape. Phylogeographic studies of

412 widespread bats and birds have shown low levels of genetic differentiation among eastern North

413 American populations (Gibbs, Dawson & Hobson, 2000; Kimura et al., 2002; Jones et al., 2005;

414 Turmelle, Kunz & Sorenson, 2011; Irwin, Irwin & Smith, 2011; but see Miller-Butterworth et al.,

415 2014). When present, genetic structure in these species is often restricted to broad-scale differentiation

416 between eastern and western populations on either side of the Rocky Mountains. In the case of eastern

417 red bats, evidence from museum records indicates that they most likely migrate from northern parts of

418 their range to the southeastern United States (Cryan, 2003) where they roost in trees during warmer

419 periods and may hibernate beneath leaf litter for short durations during colder temperatures (Saugey et

420 al., 1998; Moorman et al., 1999; Mormann & Robbins, 2007). However, there are summer resident

421 populations in the southeastern United States that likely do not migrate, and it is possible that there is

422 variation in migratory tendency across the range of eastern red bats, much like tricolored bats

423 (*Perimyotis subflavus*; Fraser et al., 2012). Mating likely takes place before or during migration in

424 eastern red bats (Dodd & Adkins, 2007; Cryan, 2008; Cryan et al., 2012; Solick et al., 2012), and can

425 take place before bats hibernate or during warm periods on the wintering grounds. Thus, the potential

426 for mating, and hence gene flow, among individuals that spent their summers in geographically

427 disparate areas during migration or on the wintering grounds is likely very high.

428 In most colonial temperate bat species, females are philopatric to natal nursery colonies or

429 undergo short dispersal distances to nearby colonies while mating takes place during swarming and/or

430 hibernation at distant sites that act as hotspots of gene flow between bats occupying distant roosts

431 during the summer (Kerth et al., 2003; Veith et al., 2004; Furmankiewicz & Altringham, 2007). As a

432 consequence, levels of mitochondrial differentiation (indicative of female movements) are often quite

433 high among summer maternity colonies while levels of nuclear differentiation (indicative of gene flow

434 through mating) are typically low (Castella, Ruedi & Excoffier, 2001; Bilgin et al., 2008; Kerth et al.,

435 2008; Vonhof, Strobeck & Fenton, 2008; Bryja et al., 2009; Lack, Wilkinson & van den Bussche,

436 2010; Turmelle, Kunz & Sorenson, 2011). Eastern red bats and other members of the genus *Lasiurus*

437 roost solitarily in foliage during the summer (Shump & Shump, 1982a,b), and if they exhibited

438 philopatry it would likely occur within broader landscape units such as forest patches or stands rather

439 than a single roost. The absence of significant mitochondrial differentiation among samples of eastern

440 red bats suggests that females may be exhibiting high levels of dispersal, and that gene flow likely

441 takes place via both male and female movements and mating (e.g., Russell, Medellín & McCracken,

442 2005; Vonhof, Strobeck & Fenton, 2008).

443 Before undertaking our study, we had no prior knowledge of whether the eastern red bat was

444 divided into a series of discrete subpopulations, possibly undertaking migration along different

445 pathways and possibly varying in size, or whether it functioned as a single, panmictic population of

446 unknown size. Our estimates of N_e varied considerably (over an order of magnitude) among the

447 different approaches we used, ranging from 7.45×10^4 based on microsatellite genotypes only (msvar),

448   to 1.52×10^6 for sequence data only (CHY in Lamarc), with intermediate estimates of 5.18×10^5 for

449   HV2 (Lamarc) and 5.91×10^5 using all markers combined (IMa2). This variation is the result of

450   methodological differences among the approaches we used, which all utilize different aspects of the

451   data and make varying assumptions about the underlying historical population processes that may have

452   occurred. Further, the analyses each used different marker data, which vary in their mutation rates, and

453   so are providing estimates across varying time scales. Nevertheless, in combination with the results of

454   population structure analyses, our data indicate that eastern red bats form a single, large, panmictic

455   population across their range and that minimum effective population sizes are likely in the hundreds of

456   thousands.

457   The parameter most relevant to management of this species, the actual number of individuals in

458   the population (N_c), is not obtainable from our estimates of N_e. A variety of factors may reduce N_e

459   relative to N_c, including fluctuations in population size over time, overlapping generations, and

460   variation among individuals in reproductive success. Attempts have been made to compare estimates of

461   N_e to N_c, and across a wide range of organisms the average N_e / N_c ratio is $0.11 - 0.14$ (Frankham,

462   1995; Palstra & Ruzzante, 2008); for mammals alone, the average ratio is 0.34 (Frankham, 1995). If we

463   applied this latter mean ratio (0.34) to our point estimates of N_e, we would obtain N_c estimates of 2.19

464    $\times 10^5$ to 4.5×10^6 individuals. However, there are a number of serious problems with the use of our

465   coalescent estimates in this way. N_e is a theoretical concept that relates the genetic characteristics of a

466   population to those expected of an ideal population under a Wright-Fisher model. We can evaluate N_e

467   as a measure of the evolutionary potential of populations, but there is no clear relationship between

468   current demography and changes in genetic variation that influence coalescent estimates of N_e. Further,

469   there are a number of methodological concerns. First, N_e has most often been estimated for very small

470   populations of less than 1,000 individuals, and we do not know how the N_e / N_c ratio may vary with the

471   magnitude of N_c. Second, the majority of the ratios provided by Frankham (1995) utilize demographic,

472   rather then genetic, estimates of N_e, and demographic estimates may differ substantially from genetic

473   estimates even when population sizes are small (Luikart et al., 2010). Third, the majority of estimates

474   in Frankham (1995) come from organisms with very different life histories than bats, and we do not

475   know to what extent the N_e / N_c ratio might vary from the overall mean for bats (or most other

476   organisms). Fourth, the calculation of N_e using coalescent-based methods requires division of estimates

477   of θ by the mutation rate (μ) to obtain values of N_e, but mutation rates are extremely difficult to

478   estimate and few good estimates exist for any gene (Ho et al., 2006; Montooth & Rand, 2008; Nabholz,

479   Glémin & Galtier, 2009), much less for any bat species. As a result, any inaccuracy in the mutation rate

480   estimate is amplified arithmetically in the subsequent calculation of N_e (Ovenden et al., 2007; Luikart

481   et al., 2010). Therefore, applying a standard conversion to convert N_e to N_c is highly problematic, and it

482   is best to use our estimates to indicate relative orders of magnitude of bat population sizes rather than

483   to provide any specific population size estimates.

484   The potential value of our estimates of N_e is that they may be used as a baseline for future

485   monitoring. Assuming fatality rates at wind turbines remain high and continue to grow as wind energy

486   development continues, it is possible that regular estimates of N_e could be utilized to document

487   population trends of affected species (Antao, Perez-Figueroa & Luikart, 2011). Regional projections of

488   bat fatalities predict annual fatality rates numbering in the tens of thousands (Kunz et al., 2007), and

489   the total number of fatalities is likely to continue to rise as wind power development expands.

490   However, the loss of genetic variation from populations and declines in N_e estimates based on linkage

491   disequilibrium are only apparent when population sizes are very small (e.g., Waples & Do, 2010),

492   suggesting that cumulative population declines may have to be very severe before they affect genetic

493   estimates. Had our estimates of N_e been considerably smaller, or had we detected numerous

494   subpopulations among which gene flow was restricted, then there may have been greater potential to

495   document population size changes using genetic approaches. Given our results supporting a large,

496   panmictic population, simulation studies are required to assess the sensitivity of coalescent-based

497   estimates of N_e to population decline and to assess the utility of this approach for eastern red bats.

498   Our genetic data indicating panmixia and a lack of evidence for the use of different migratory

499   pathways in different parts of the range highlights the need to consider the global implications of

500   current and future fatalities associated with wind power. Despite growing conservation concern,

501   current monitoring of bat fatalities at wind power developments is performed on an ad-hoc, site-by-site

502   basis and may vary tremendously in scope according to local regulations. While such monitoring can

503   provide valuable insights leading to site-level mitigation strategies or changes in turbine placement in

504   some cases, biologists lack the necessary broader context within which to assess the long term,

505   population-level impacts of observed fatality rates and management strategies at specific sites. For

506   instance, site-specific, per-turbine thresholds to limit fatalities through curtailment (reducing turbine

507   blade speed and operating time on low-wind nights in summer and fall to decrease fatalities; Baerwald

508   et al., 2009; Arnett et al., 2011) ignore the fact that the demographic consequences of mortality extend

509   well beyond any particular jurisdiction. Evidence from stable isotopes indicates that bats killed at wind

510   power developments may originate from wide geographic areas (Voigt et al., 2012; Baerwald et al.,

511   2014), and thus mortality at any given site can impact bat populations using geographically widespread

512   catchment areas. Given that observed bat fatality rates at wind power facilities vary considerably

513   among sites and regions (Arnett et al., 2008), our findings underscore the need for better data

514   integration across jurisdictions and monitoring programs to adequately assess the cumulative

515   demographic and genetic impacts of continued fatalities.

516

517   **ACKNOWLEDGEMENTS**

We are grateful to S. Amelon, R. Benedict, E. Britzke, D. Brown, C. Butchkoski, T. Carter, S.

Castleberry, M. K. Clark, S. Darling, J. Fiedler, L. Finn, B. French, E. Gates, J. Gore, M. Gumbert, G.

Johnson, J. Johnson, J. Kiser, S. Lambiase, G. Libby, K. Luzynski, A. Miles, J. O'Keefe, E. Pannkuk,

R. Perry, L. Pruitt, L. Reddy, H. Rice, L. Robbins, D. Saugey, M. Schirmacher, J. Schwierjohann, D.

Sparks, C. Stihler, V. Swier, A. Tibbels, W. Tidhar, C. Willis, and L. Winhold, and to the Angelo State

Natural History Collection, the Tennessee State Rabies Testing Lab, and the Carnegie Museum of

Natural History for providing tissue samples to support this research. J. Glatz kindly provided GIS

expertise to produce the range map. We also thank the Bats and Wind Energy Cooperative, and

particularly E. Arnett, C. Hein, and W. Frick for their input and support.

REFERENCES

Abbasi T, Premalatha M, Abbasi T, Abbasi SA. 2014. Wind Energy: Increasing Deployment, Rising
Environmental Concerns. *Renewable and Sustainable Energy Reviews* **31:**270-288 DOI
10.1016/j.rser.2013.11.019.

Antao T, Perez-Figueroa A, Luikart G. 2011. Early detection of population declines: high power of
genetic monitoring using effective population size estimators. Evolutionary Applications 4:
144-154.

**Arnett EA, Brown WK, Erickson WP, Fiedler JK, Hamilton BL, Henry TH, Jain A, Johnson
GD, Kerns J, Koford RR, Nicholson CP, O'Connell TJ, Piorkowski MD, Tankersley RD.
2008.** Patterns of Bat Fatalities at Wind Energy Facilities in North America. *Journal of Wildlife
Management* **72:**61-78 DOI 10.2193/2007-221.

Arnett EA, Huso MMP, Schirmacher MR, Hayes JP. 2011. Altering turbine speed reduces bat
mortality at wind-energy facilities. *Frontiers in Ecology and the Environment* **9:**209-214.

Avise JC. 2000. *Phylogeography: The History and Formation of Species*. Harvard University Press,

542   Cambridge.

543 **Baerwald EF, Edworthy J, Holder M, Barclay RMR. 2009.** A large-scale mitigation experiment to

544   reduce bat fatalities at wind energy facilities. *Journal of Wildlife Management* **73:**1077-1081.

545 **Baerwald EF, Patterson WP, Barclay RMR. 2014.** Origins and migratory patterns of bats killed by

546   wind turbines in southern Alberta: evidence from stable isotopes. *Ecosphere* **5:**118.

547 **Beaumont MA 1999.** Detecting Population Expansion and Decline Using Microsatellites. *Genetics*

548   **153:**2013-2029.

549 **Bilgin R, Karatas A, Coraman E, Morales JC. 2008.** The Mitochondrial and Nuclear Genetic

550   Structure of *Myotis capaccinii* (Chiroptera: Vespertilionidae) in the Eurasian Transition, and Its

551   Taxonomic Implications. *Zoologica Scripta* **37:**253-262 DOI 10.1111/j.1463-

552   6409.2008.00326.x.

553 **Bryja J, Kanuch P, Fornuskova A, Bartonicka T, Rehak Z. 2009.** Low Population Genetic

554   Structuring of Two Cryptic Bat Species Suggests Their Migratory Behaviour in Continental

555   Europe. *Biological Journal of the Linnean Society* **96:**103-114 DOI 10.1111/j.1095-

556   8312.2008.01093.x.

557 **Castella V, Ruedi M, Excoffier L. 2001.** Contrasted Patterns of Mitochondrial and Nuclear Structure

558   Among Nursery Colonies of the Bat *Myotis myotis*. *Journal of Evolutionary Biology* **14:**708-

559   720 DOI 10.1046/j.1420-9101.2001.00331.x.

560 **Chapuis M-P, Estoup A. 2007.** Microsatellite Null Alleles and Estimation of Population

561   Differentiation. *Molecular Biology and Evolution* **24:**621-631.

562 **Crandall KA, Posada D, Vasco D. 1999.** Effective Population Sizes: Missing Measures and Missing

563   Concepts. *Animal Conservation* **2:**317-319 DOI 10.1111/j.1469-1795.1999.tb00078.x.

564 **Crow JF, Denniston C. 1988.** Inbreeding and Variance Effective Population Numbers. *Evolution*

565   **42:**482-495.

566 **Cryan PM. 2003.** Seasonal Distribution of Migratory Tree Bats (*Lasiurus* and *Lasionycteris*) in North

567 America. *Journal of Mammalogy* **84:**579-593 DOI http://dx.doi.org/10.1644/1545-

568 1542(2003)084<0579:SDOMTB>2.0.CO;2.

569 **Cryan PM. 2008.** Mating Behavior as a Possible Cause of Bat Fatalities at Wind Turbines. *Journal of*

570 *Wildlife Management* **72:**845-849 DOI 10.2193/2007-371.

571 **Cryan PM, Jameson JW, Baerwald EF, Willis CKR, Barclay RMR, Snider EA, Crichton EG.**

572 **2012.** Evidence of Late-Summer Mating Readiness and Early Sexual Maturation in Migratory

573 Tree-Roosting Bats Found Dead at Wind Turbines. *PLoS ONE* **7:**e47586 DOI

574 10.1371/journal.pone.0047586.

575 **Dodd LE, Adkins JK. 2007.** Observations of Mating Behavior in the Eastern Red Bat (*Lasiurus*

576 *borealis*). *Bat Research News* **44:**155-156.

577 **Duchesne P, Turgeon J. 2009.** FLOCK: a method for quick mapping of admixture without source

578 samples. *Molecular Ecology Resources* **9**:1333-1344.

579 **Duchesne P, Turgeon J. 2012.** FLOCK Provides Reliable Solutions to the "Number of Populations"

580 Problem. *Journal of Heredity* **103:**734-743 DOI 10.1093/jhered/ess038.

581 **Earl DA, vonHoldt BM. 2012.** STRUCTURE HARVESTER: A Website and Program for Visualizing

582 STRUCTURE Output and Implementing the Evanno Method. *Conservation Genetics*

583 *Resources* **4:**359-361 DOI 10.1007/s12686-011-9548-7.

584 **Erickson WP, Johnson GD, Strickland MD, Young DP, Sernka KJ, Good RE. 2001.** Avian

585 Collisions with Wind Turbines: A Summary of Existing Studies and Comparisons to Other

586 Sources of Avian Collision Mortality in the United States. National Wind Coordinating

587 Committee Research Document, Washington, DC.

588 **Erickson WP, Johnson GD, Young DP. 2005.** A Summary and Comparison of Bird Mortality from

589 Anthropogenic Causes with an Emphasis on Collisions. In: Ralph CJ, Rich TD, eds. *Bird*

590   *Conservation Implementation and Integration in the Americas: Proceedings of the Third*

591   *International Partners in Flight Conference*. Albany, CA: USDA Forest Service Pacific

592   Southwest Research Station, 1029-1042.

593 **Evanno G, Regnaut S, Goudet J. 2005.** Detecting the Number of Clusters of Individuals Using the

594   Software STRUCTURE: A Simulation Study. *Molecular Ecology* **14:**2611-2620 DOI

595   10.1111/j.1365-294X.2005.02553.x.

596 **Excoffier L, Laval G, Schneider S. 2005.** Arlequin (Version 3.0): An Integrated Software Package for

597   Population Genetics Data Analysis. *Evolutionary Bioinformatics Online* **1:**47-50.

598 **Excoffier L, Smouse PE, Quattro JM. 1992.** Analysis of Molecular Variance Inferred from Metric

599   Distances among DNA Haplotypes: Application to Human Mitochondrial DNA Restriction

600   Data. *Genetics* **131:**479-491.

601 **Falush D, Stephens M, Pritchard JK. 2003.** Inference of Population Structure Using Multilocus

602   Genotype Data: Linked Loci and Correlated Allele Frequencies. *Genetics* **164:**1567-1587.

603 **Felsenstein J. 2006.** Accuracy of Coalescent Likelihood Estimates: Do We Need More Sites, More

604   Sequences, or More Loci? *Molecular Biology and Evolution* **23:**691-700.

605 **Frankham R. 1995.** Effective Population Size/Adult Population Size Ratios in Wildlife: A Review.

606   *Genetical Research* **66:**95-107 DOI: http://dx.doi.org/10.1017/S0016672300034455.

607 **Frankham R, Ballou JD, Briscoe DA. 2002.** *Introduction to Conservation Genetics*. Cambridge, UK:

608   Cambridge University Press.

609 **Fraser EE, McGuire LP, Eger JL, Longstaffe FJ, Fenton MB. 2012.** Evidence of Latitudinal

610   Migration in Tri-Colored Bats, *Perimyotis subflavus*. *PLoS ONE* **7:**e31419 DOI

611   10.1371/journal.pone.0031419.

612 **Freeland JR, Petersen SD, Kirk H. 2011.** *Molecular Ecology, 2nd Edition*. Wiley-Blackwell, Oxford.

613 **Furmankiewicz J, Altringham J. 2007.** Genetic Structure in a Swarming Brown Long-Eared Bat

614   (*Plecotus auritus*) Population: Evidence for Mating at Swarming Sites. *Conservation Genetics*

615   **8:**913-923 DOI 10.1007/s10592-006-9246-2.

616 **Gibbs HL, Dawson RJG, Hobson KA. 2000.** Limited Differentiation in Microsatellite DNA

617   Variation among Northern Populations of the Yellow Warbler: Evidence for Male-Biased Gene

618   Flow? *Molecular Ecology* **9:**2137-2147 DOI 10.1046/j.1365-294X.2000.01136.x.

619 **Glass BP. 1982.** Seasonal Movements of Mexican Freetail Bats *Tadarida brasiliensis mexicana*

620   Banded in the Great Plains. *Southwestern Naturalist* **27:**127–133.

621 **Goudet J. 1995.** FSTAT (Version 1.2): A Computer Program to Calculate *F*-Statistics. *Journal of*

622   *Heredity* **86:**485-486.

623 **Guillot G, Leblois R, Coulon A, Frantz AC. 2009.** Statistical Methods in Spatial Genetics. *Molecular*

624   *Ecology* **18:**4734-4756 DOI 10.1111/j.1365-294X.2009.04410.x.

625 **Hey J. 2010a.** The Divergence of Chimpanzee Species and Subspecies as Revealed in Multipopulation

626   Isolation-with-Migration Analyses. *Molecular Biology and Evolution* **27:**921-933 DOI

627   10.1093/molbev/msp298.

628 **Hey J. 2010b.** Isolation with Migration Models for More Than Two Populations. *Molecular Biology*

629   *and Evolution* **27:**905-920 DOI 10.1093/molbev/msp296.

630 **Ho SYW, Phillips MJ, Cooper A, Drummond AJ. 2006.** Time Dependency of Molecular Rate

631   Estimates and Systematic Overestimation of Recent Divergence Times. *Molecular Biology and*

632   *Evolution* **22:**1561-1568 DOI 10.1093/molbev/msi145.

633 **Hubisz MJ, Falush D, Stephens M, Pritchard JK. 2009.** Inferring Weak Population Structure with

634   the Assistance of Sample Group Information. *Molecular Ecology Resources* **9:**1322-1332 DOI

635   10.1111/j.1755-0998.2009.02591.x.

636 **Irwin DE, Irwin JH, Smith TB. 2011.** Genetic Variation and Seasonal Migratory Connectivity in

637   Wilson's Warblers (*Wilsonia pusilla*): Species-Level Differences in Nuclear DNA Between

638   Western and Eastern Populations. *Molecular Ecology* **20**:3102-3115 DOI 10.1111/j.1365-

639   294X.2011.05159.x.

640   **Jones KL, Krapu GL, Brandt DA, Ashley MV. 2005.** Population Genetic Structure in Migratory

641   Sandhill Cranes and the Role of Pleistocene Glaciations. *Molecular Ecology* **14:**2645-2657

642   DOI 10.1111/j.1365-294X.2005.02622.x.

643   **Jorde PE, Ryman N. 1995.** Temporal Allele Frequency Change and Estimation of Effective Size in

644   Populations with Overlapping Generations. *Genetics* **139:**1077–1090.

645   **Jost L. 2008.** G_{ST} and Its Relatives Do Not Measure Differentiation. *Molecular Ecology* **17:**4015-4026

646   DOI 10.1111/j.1365-294X.2008.03887.x.

647   **Kaldellis JK, Zafirakis D. 2011.** The Wind Energy (R)evolution: A Short Review of a Long History.

648   *Renewable Energy* **36**:1887-1901.

649   **Kalinowski ST. 2005.** HP-RARE 1.0: A Computer Program for Performing Rarefaction on Measures

650   of Allelic Richness. *Molecular Ecology Notes* **5:**187-189 DOI 10.1111/j.1471-

651   8286.2004.00845.x.

652   **Kalinowski ST, Taper ML, Marshall TC. 2007.** Revising how the Computer Program CERVUS

653   Accommodates Genotyping Error Increases Success in Paternity Assignment. *Molecular*

654   *Ecology* **16**:1099-1106.

655   **Kerth G, Kiefer A, Trappmann C, Weishaar M. 2003.** High Gene Diversity at Swarming Sites

656   Suggest Hot Spots for Gene Flow in the Endangered Bechstein's Bat. *Conservation Genetics*

657   **4:**491-499.

658   **Kerth G, Petrov B, Conti A, Anastasov D, Weishaar M, Gazaryan S, Jaquiéry J, König B, Perrin**

659   **N, Bruyndonckx N. 2008.** Communally Breeding Bechstein's Bats Have a Stable Social

660   System That Is Independent from the Postglacial History and Location of the Populations.

661   *Molecular Ecology* **17:**2368-2381 DOI 10.1111/j.1365-294X.2008.03768.x.

662 **Kimura M, Clegg SM, Lovette IJ, Holder KR, Girman DJ, Milá B, Wade P, Smith TB. 2002.**

663   Phylogeographical Approaches to Assessing Demographic Connectivity Between Breeding and

664   Overwintering Regions in a Nearctic-Neotropical Warbler (*Wilsonia pusilla*). *Molecular*

665   *Ecology* **11:**1605-1616 DOI 10.1046/j.1365-294X.2002.01551.x.

666 **Kuhner MK. 2006.** LAMARC 2.0: Maximum Likelihood and Bayesian Estimation of Population

667   Parameters. *Bioinformatics* **22:**768-770 DOI 10.1093/bioinformatics/btk051.

668 **Kunz TH. 1982.** *Lasionycteris noctivagans*. *Mammalian Species* **172:**1-5.

669 **Kunz TH, Arnett EB, Erickson WP, Hoar AR, Johnson GD, Larkin RP, Strickland MD,**

670   **Thresher RW, Tuttle MD. 2007.** Ecological Impacts of Wind Energy Development on Bats:

671   Questions, Research Needs, and Hypotheses. *Frontiers in Ecology and the Environment* **5:**315-

672   324 DOI http://dx.doi.org/10.1890/1540-9295(2007)5[315:EIOWED]2.0.CO;2.

673 **Kunz TH, Betke M, Hristov N, Vonhof MJ. 2009.** Methods for Assessing Abundance of Bats. In:

674   Kunz TH, Parsons S, eds. *Behavioral and Ecological Methods for the Study of Bats, 2nd Ed.*

675   Baltimore, MD: Johns Hopkins University Press, 133-157.

676 **Lack JB, Wilkinson JE, van den Bussche RA. 2010.** Range-Wide Population Genetic Structure of

677   the Pallid Bat (*Antrozous pallidus*) − Incongruent Results from Nuclear and Mitochondrial

678   DNA. *Acta Chiropterologica* **12:**401-413 DOI http://dx.doi.org/10.3161/150811010X537981.

679 **Leberg P. 2005.** Genetic Approaches for Estimating the Effective Size of Populations. *Journal of*

680   *Wildlife Management* **69:**1385-1399 DOI http://dx.doi.org/10.2193/0022-

681   541X(2005)69[1385:GAFETE]2.0.CO;2.

682 **Leung DYC, Yang Y. 2012.** Wind energy Development and its Environmental Impact: A Review.

683   *Renewable and Sustainable Energy Reviews* **16:**1031-1039.

684 **Librado P, Rozas J. 2009.** DnaSP v5: A Software for Comprehensive Analysis of DNA

685   Polymorphism Data. *Bioinformatics* **25:**1451-1452 DOI 10.1093/bioinformatics/btp187.

686   **Luikart G, Ryman N, Tallmon DA, Schwartz MK, Allendorf FW. 2010.** Estimation of Census and

687   Effective Population Sizes: The Increasing Usefulness of DNA-Based Approaches.

688   *Conservation Genetics* **11:**355-373 DOI 10.1007/s10592-010-0050-7.

689   **Meirmans PG. 2012.** AMOVA-Based Clustering of Population Genetic Data. *Journal of Heredity*

690   **103:**744-750 DOI 10.1093/jhered/ess047.

691   **Miller-Butterworth CM, Vonhof MJ, Rosenstern J, Turner GG, Russell AL. 2014.** Genetic

692   Structure of Little Brown Bats (*Myotis lucifugus*) Corresponds with Spread of White-Nose

693   Syndrome Among Hibernacula. *Journal of Heredity* **105:**354-364 DOI 10.1093/jhered/esu012.

694   **Montooth KL, Rand DM. 2008.** The Spectrum of Mitochondrial Mutation Differs Across Species.

695   *PLoS Biology* **6:**e213 DOI 10.1371/journal.pbio.0060213.

696   **Moorman CE, Russell KR, Menzel MA, Lohr SM, Ellenberger JE, Van Lear DH. 1999.** Bats

697   Roosting in Deciduous Leaf Litter. *Bat Research News* **40:**74–75.

698   **Mormann BM, Robbins LW. 2007.** Winter Roosting Ecology of Eastern Red Bats in Southwest

699   Missouri. *Journal of Wildlife Management* **71:**213-217 DOI 10.2193/2005-622.

700   **Morrison ML, Sinclair AK. 2004.** Environmental Impacts of Wind Energy Technology.

701   *Encyclopedia of Energy* **6:**435-448.

702   **Nabholz B, Glémin S, Galtier N. 2009.** The Erratic Mitochondrial Clock: Variations of Mutation

703   Rate, Not Population Size, Affect MtDNA Diversity Across Birds and Mammals. *BMC*

704   *Evolutionary Biology* **9:**e54 DOI 10.1186/1471-2148-9-54.

705   **O'Shea TJ, Bogan MA. 2003.** *Monitoring Trends in Bat Populations of the United States and*

706   *Territories: Problems and Prospects*. Springfield, VA: US Geological Survey.

707   **Ovenden JR, Peel D, Street R, Courtney AJ, Hoyle SD, Peel SL, Podlich H. 2007.** The Genetic

708   Effective and Adult Census Size of an Australian Population of Tiger Prawns (*Penaeus*

709   *esculentus*). *Molecular Ecology* **16:**127–138 DOI 10.1111/j.1365-294X.2006.03132.x.

710 **Oyler-McCance SJ, Fike JA. 2011.** Characterization of Small Microsatellite Loci Isolated in

711   Endangered Indiana Bat (*Myotis sodalis*) for Use in Non-Invasive Sampling. *Conservation*

712   *Genetics Resources* **3:**243-245 DOI 10.1007/s12686-010-9332-0.

713 **Palstra FP, Ruzzante DE. 2008.** Genetic Estimates of Contemporary Effective Population Size: What

714   Can They Tell Us About the Importance of Genetic Stochasticity for Wild Population

715   Persistence? *Molecular Ecology* **17:**3428-3447 DOI 10.1111/j.1365-294X.2008.03842.x.

716 **Pesole G, Gissi C, De Chirico A, Saccone C. 1999.** Nucleotide Substitution Rate of Mammalian

717   Mitochondrial Genomes. *Journal of Molecular Evolution* **48:**427-434.

718 **Piaggio AJ, Figueroa JA, Perkins SL. 2009.** Development and Characterization of 15 Polymorphic

719   Microsatellite Loci Isolated from Rafinesque's Big-Eared Bat, *Corynorhinus rafinesquii.*

720   *Molecular Ecology Resources* **9:**1191-1193 DOI 10.1111/j.1755-0998-2009-02625.x.

721 **Piaggio AJ, Miller KEG, Matocq MD, Perkins SL. 2009.** Eight Polymorphic Microsatellite Loci

722   Developed and Characterized from Townsend's Big-Eared Bat, *Corynorhinus townsendii*.

723   *Molecular Ecology Resources* **9:**258-260 DOI 10.1111/j.1755-0998-2008-02243.x.

724 **Pritchard JK, Stephens M, Donnelly P. 2000.** Inference of Population Structure Using Multilocus

725   Genotype Data. *Genetics* **155:**945-959.

726 **Rivers NM, Butlin RK, Altringham JD. 2006.** Autumn Swarming Behaviour of Natterer's Bats in the

727   UK: Population Size, Catchment Area and Dispersal. *Biological Conservation* **127:**215-226

728   DOI 10.1016/j.biocon.2005.08.010.

729 **Russell AL, Medellín RA, McCracken GF. 2005.** Genetic Variation and Migration in the Mexican

730   Free-Tailed Bat (*Tadarida brasiliensis mexicana*). *Molecular Ecology* **14:**2207-2222 DOI

731   10.1111/j.1365-294X.2005.02552.x.

732 **Russell AL, Cox MP, Brown VA, McCracken GF. 2011.** Population Growth of Mexican Free-Tailed

733   Bats (*Tadarida brasiliensis mexicana*) Predates Human Agricultural Activity. *BMC*

734   *Evolutionary Biology* **11:**e88 DOI 10.1186/1471-2148-11-88.

735   **Saugey DA, Crump BG, Vaughn RL, Heidt GA. 1998.** Notes on the natural history of *Lasiurus*

736   *borealis* in Arkansas. *Journal of the Arkansas Academy of Science* **52:**92–98.

737   **Shump KA, Shump AU. 1982a.** *Lasiurus borealis. Mammalian Species* **183:**1-6.

738   **Shump KA, Shump AU. 1982a.** *Lasiurus cinereus. Mammalian Species* **185:**1-5.

739   **Solick DI, Gruver JC, Clement MJ, Murray KL, Courage Z. 2012.** Mating Eastern Red Bats Found

740   Dead at a Wind-Energy Facility. *Bat Research News* **53:**15-18.

741   **Stephens M, Donnelly P. 2003.** A Comparison of Bayesian Methods for Haplotype Reconstruction.

742   *American Journal of Human Genetics* **73:**1162-1169 DOI 10.1086/379378.

743   **Stephens M, Smith NJ, Donnelly P. 2001.** A New Statistical Method for Haplotype Reconstruction

744   from Population Data. *American Journal of Human Genetics* **68:**978-989 DOI 10.1086/319501.

745   **Storz JF, Beaumont MA. 2002.** Testing for Genetic Evidence of Population Expansion and

746   Contraction: An Empirical Analysis of Microsatellite DNA Variation Using a Hierarchical

747   Bayesian Model. *Evolution* **56:**154-166 DOI 10.1111/j.0014-3820.2002.tb00857.x.

748   **Tallmon DA, Koyuk A, Luikart G, Beaumont MA. 2008.** ONeSAMP: A Program to Estimate

749   Effective Population Size Using Approximate Bayesian Computation. *Molecular Ecology*

750   *Resources* **8:**299-301 DOI 10.1111/j.1471-8286.2007.01997.x.

751   **Tallmon DA, Luikart G, Beaumont MA. 2004.** Comparative Evaluation of a New Effective

752   Population Size Estimator Based on Approximate Bayesian Computation. *Genetics* **167:**977-

753   988 DOI 10.1534/genetics.103.026146.

754   **Trujillo RG, Amelon SK. 2009.** Development of Microsatellite Markers in *Myotis sodalis* and Cross-

755   Species Amplification in *M. grisescens*, *M. leibii*, *M. lucifugus*, and *M. septentrionalis*.

756   *Conservation Genetics* **10:**1965-1968 DOI 10.1007/s10592-009-9869-1.

757   **Turmelle AS, Kunz TH, Sorenson MD. 2011.** A Tale of Two Genomes: Contrasting Patterns of

758   Phylogeographic Structure in a Widely Distributed Bat. *Molecular Ecology* **20:**357-375 DOI

759   10.1111/j.1365-294X.2010.04947.x.

760 **Veith M, Beer N, Kiefer A, Johannesen J, Seitz A. 2004.** The Role of Swarming Sites for

761   Maintaining Gene Flow in the Brown Long-Eared Bat (*Plecotus auritus*). *Heredity* **93:**342-349

762   DOI 10.1038/sj.hdy.6800509.

763 **Venta PJ, Brouillette JA, Yuzbasiyan-Gurkan V, Brewer GJ. 1996.** Gene-Specific Universal

764   Mammalian Sequence-Tagged Sites: Application to the Canine Genome. *Biochemical Genetics*

765   **34:**321-341.

766 **Voigt CC, Popa-Lisseanu AG, Niermann I, Kramer-Schadt S. 2012.** The catchment area of wind

767   farms for European bats: a plea for international regulations. *Biological Conservation* **153**:80-

768   86.

769 **Vonhof MJ, Strobeck C, Fenton MB. 2008.** Genetic Variation and Population Structure in Big

770   Brown Bats (*Eptesicus fuscus*): Is Female Dispersal Important? *Journal of Mammalogy*

771   **89:**1411-1420 DOI http://dx.doi.org/10.1644/08-MAMM-S-062.1.

772 **Wang J. 2005.** Estimation of Effective Population Sizes from Data on Genetic Markers. *Philosophical*

773   *Transactions of the Royal Society B* **360:**1395-1409 DOI 10.1098/rstb.2005.1682.

774 **Waples RS, Do C. 2009.** LDNE: A Program for Estimating Effective Population Size from Data on

775   Linkage Disequilibrium. *Molecular Ecology Resources* **8:**753-756 DOI 10.1111/j.1755-

776   0998.2007.02061.x.

777 **Waples RS, Do C. 2010.** Linkage Disequilibrium Estimates of Contemporary N_e Using Highly

778   Variable Genetic Markers: A Largely Untapped Resource for Applied Conservation and

779   Evolution. *Evolutionary Applications* **3:**244-262 DOI 10.1111/j.1752-4571.2009.00104.x.

780 **Weir BS, Cockerham CC. 1984.** Estimating *F*-Statistics for the Analysis of Population Structure.

781   *Evolution* **38:**1358-1370.

782   **Wilkinson GS, Chapman AM. 1991.** Length and Sequence Variation in Evening Bat D-Loop

783   MtDNA. *Genetics* **128:**607-617.

784

785

Sites sampled and diversity statistics for 16-locus microsatellite genotypes and mitochondrial HV2 sequences.

Site labels represent two-letter state codes as in Figure 1. N_{Gen} = number of individuals genotyped, N_A = number of alleles, H_O = observed heterozygosity, H_E = expected heterozygosity, AR = allelic richness, AR_{Priv} = private allelic richness, F_{IS} = inbreeding coefficient, N_{Seq} = number of individuals sequenced at mitochondrial HV2 locus, N_H = number of haplotypes, h = haplotype diversity, π = nucleotide diversity. Overall values represent means for all measures except N_{Gen} and N_{Seq}, which represent sums.

Site	State or Province	N_{Gen}	N_A	H_O	H_E	AR	AR_{Priv}	F_{IS}	N_{Seq}	N_H	h	π
AR	Arkansas	39	18.25	0.84	0.88	13.14	0.50	0.044	25	21	0.987	0.016
GA	Georgia	30	16.75	0.81	0.87	13.12	1.16	0.064	17	13	0.963	0.009
IL	Illinois	26	15.31	0.80	0.87	12.88	0.56	0.084	26	22	0.985	0.013
MD	Maryland	21	13.31	0.81	0.86	12.19	0.80	0.057	15	15	1.000	0.012
MI	Michigan	17	12.69	0.82	0.88	12.69	0.84	0.073	16	16	1.000	0.013
MO	Missouri	27	16.25	0.84	0.89	13.20	0.80	0.056	34	21	0.961	0.009
NC	North Carolina	18	13.19	0.81	0.88	12.87	0.76	0.079				
ON	Ontario	19	14.13	0.87	0.88	13.43	1.05	0.021	19	17	0.983	0.012
TN	Tennessee	22	14.50	0.82	0.87	12.98	0.79	0.065	26	23	0.991	0.010
TX	Texas	20	14.19	0.79	0.88	13.14	0.81	0.105	21	20	0.995	0.011
WV-Pe	West Virginia	20	13.25	0.83	0.87	12.35	0.79	0.050	19	18	0.994	0.010
WV-Ma	West Virginia	25	15.44	0.85	0.88	13.02	0.45	0.036				
Overall		**284**	**14.77**	**0.82**	**0.88**	**12.92**	**0.78**	**0.061**	**218**	**18.6**	**0.986**	**0.011**

Pairwise F_{ST} (below diagonal) and Jost's D (above diagonal) values based on 16-locus microsatellite genotypes.

No pairwise F_{ST} values were significant based on 10,000 permutations.

Site	AR	GA	IL	MD	MI	MO	NC	ON	TN	TX	WV-Pe	WV-Ma
AR	-	0.027	0.02	0.001	0.013	0.018	0.001	-0.025	0.025	0.033	0.025	0.001
GA	0.004	-	0.041	0.02	0.039	0.068	0.011	0.027	0.029	0.047	0.054	0.029
IL	0.003	0.006	-	0.026	0.046	0.037	0.011	0.007	0.018	0.055	0.037	0.026
MD	0	0.003	0.004	-	0.012	0.022	0.035	0.009	0.012	0.041	0.02	-0.022
MI	0.002	0.006	0.007	0.002	-	0.001	-0.033	0.012	0.015	0.012	0.021	0.026
MO	0.003	0.009	0.005	0.003	0	-	0.006	0.015	0.052	0.049	0.013	0.006
NC	0	0.002	0.002	0.005	-0.004	0.001	-	-0.017	0.02	-0.002	0.018	0.003
ON	-0.003	0.004	0.001	0.001	0.002	0.002	-0.002	-	0.026	-0.036	0.024	0.023
TN	0.004	0.004	0.003	0.002	0.002	0.007	0.003	0.004	-	0.031	0.029	0.026
TX	0.005	0.007	0.008	0.006	0.002	0.006	0	-0.005	0.004	-	0.021	0.039
WV-Pe	0.004	0.008	0.005	0.003	0.003	0.002	0.002	0.003	0.004	0.003	-	0.011
WV-Ma	0	0.004	0.004	-0.003	0.004	0.001	0.001	0.003	0.004	0.006	0.002	-

4

Pairwise F_{ST} values based on mitochondrial HV2 sequence data.

Significant values based on 10,000 permutations ($P < 0.05$) are denoted with an *.

Site	AR	GA	IL	MD	MI	MO	ON	TN	TX
AR	-								
GA	0.012	-							
IL	-0.008	0.032	-						
MD	0.014	0.037	0.019	-					
MI	-0.006	-0.006	0.006	-0.011	-				
MO	0.024	0.021	0.037*	0.032	0.016	-			
ON	0.005	0.014	-0.005	0.008	0.000	-0.006	-		
TN	0.006	0.009	0.001	0.030	0.005	0.008	-0.004	-	
TX	0.028	0.049	0.042*	0.021	0.020	0.013	0.000	0.036	-
WV-Pe	0.003	0.015	-0.001	0.014	0.005	-0.009	-0.030	-0.016	0.009

4

Estimates of θ, N_e, and population growth (g) based on Lamarc analyses.

	θ (95% CI)	N_e (95% CI)	g (95% CI)
HV2			
Run 1	0.022 (0.018, 0.031)	5.0×10^5 ($4.16 - 7.26 \times 10^5$)	964.25 (361.03, 1007.18)
Run 2	0.024 (0.019, 0.029)	5.52×10^5 ($4.33 - 6.78 \times 10^5$)	965.75 (358.34, 1007.50)
Run 3	0.022 (0.018, 0.033)	5.0×10^5 ($4.25 - 7.61 \times 10^5$)	965.95 (382.04, 1006.35)
Overall	0.022 (0.018, 0.031)	5.18×10^5 ($4.25 - 7.22 \times 10^5$)	965.32 (367.14, 1007.01)
CHY			
Run 1	0.048 (0.033, 0.067)	1.54×10^6 ($1.07 - 2.15 \times 10^6$)	958.85 (496.01, 1002.27)
Run 2	0.046 (0.032, 0.067)	1.50×10^6 ($1.03 - 2.17 \times 10^6$)	957.10 (486.19, 1002.01)
Run 3	0.047 (0.033, 0.069)	1.52×10^6 ($1.06 - 2.21 \times 10^6$)	952.73 (479.76, 1001.04)
Overall	0.047 (0.033, 0.068)	1.52×10^6 ($1.05 - 2.18 \times 10^6$)	956.23 (487.32, 1001.77)

4

Estimates of current and ancestral N_e, time of growth and population trend based on msvar analyses.

Year	Current N_e (mode ± variance)	Ancestral N_e (mode ± variance)	Time of growth (mode ± variance)	Trend
2002_A1	125,786 ± 4.9	24,191 ± 4.5	5,353 ± 1.9	Growth
2002_A2	21,120 ± 6.2	57,497 ± 3.1	6,924 ± 1.9	Decline
2002_A3	106,925 ± 3.3	22,460 ± 6.0	27,256 ± 5.8	Growth
2002_B1	137,848 ± 6.1	14,626 ± 4.6	11,710 ± 3.3	Growth
2002_B3	195,164 ± 4.4	651,754 ± 3.1	21,915 ± 1.1	Decline
2010_A1	46,279 ± 3.5	59,872 ± 2.6	88,776 ± 1.9	Decline
2010_A2	36,766 ± 5.6	427,688 ± 3.8	16,088 ± 4.3	Decline
2010_A3	24,733 ± 2.4	44,036 ± 5.5	32,866 ± 1.6	Decline
2010_B1	22,845 ± 3.8	81,332 ± 7.6	5,161 ± 4.2	Decline
2010_B2	12,670 ± 5.4	29,191 ± 3.8	9,978 ± 1.3	Decline
2010_B3	89,050 ± 10.0	724,656 ± 2.8	11,552 ± 7.2	Decline

4

1

Figure 1. Map showing the range of eastern red bats and all sampling locations

Only labeled locations (black dots) had sufficient sample sizes to be included in population-level analyses, and labels reflect two-letter state or province codes (two sampling locations within West Virginia are further labeled with the first two letters of the county to distinguish them). The range map source is the IUCN (http://www.iucnredlist.org/details/11347/0).

2

Tukey boxplot of current N_e from msvar analyses.

Estimates are given on the $\log_{10}$ scale. Datasets A and B represent different subsamples of the full dataset from each respective year.
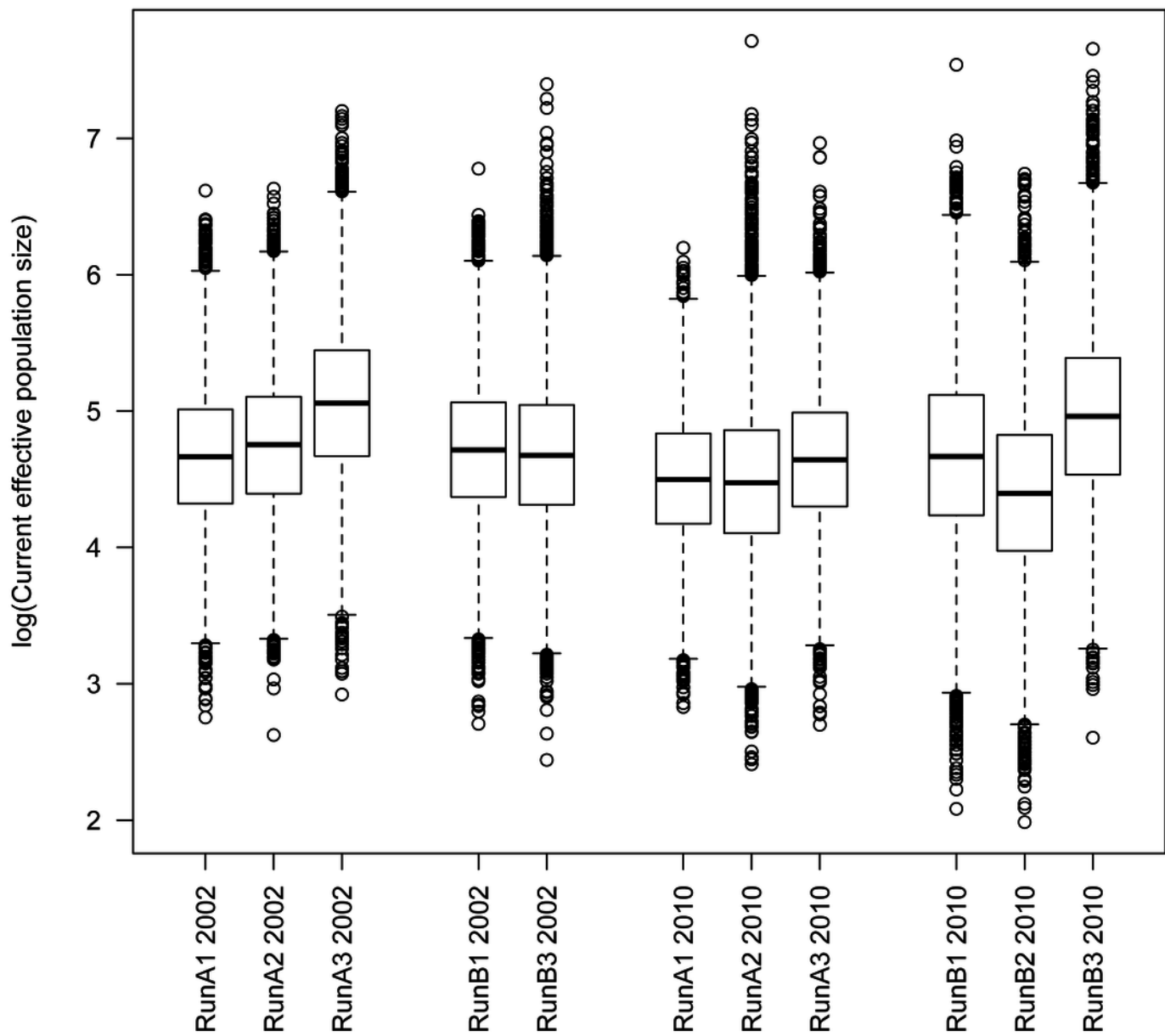
Posterior probability of N_e for eastern red bats, estimated using IMa2.

The analysis includes autosomal DNA sequence data, mitochondrial DNA sequence data, and autosomal microsatellite genotype data.